Nonlinear dielectric properties and temperature stabilization effect near the ferroelectric phase transition in sodium trihydrogen selenite

Nonlinear dielectric properties and temperature stabilization effect near the ferroelectric phase transition in sodium trihydrogen selenite

A Stankiewicz, R Cach and S Dacko

Institute of Experimental Physics, University of Wroclaw, plac Maksa Borna 9, 50-205 Wroclaw, Poland

Abstract
The ferroelectric phase transition of crystalline sodium trihydrogen selenite has been characterized by domain observations and measurements of electric permittivity, pyroeffect and spontaneous polarization. The first-order character of the phase transition is clearly demonstrated by the phase coexistence and temperature autostabilization. The considerable heating effect at 50 Hz ac field is described. The electric field effect on the temperature variation of the electric permittivity, in the phase transition region, shows a considerable domain structure contribution to the permittivity value. It is demonstrated that the dielectric properties of x- and y-samples can be described by classical dielectric state equations: the set of coefficients has been determined. It is concluded that the x-component of spontaneous polarization plays a predominant role in the phase transition.

1. Introduction

The ferroelectric properties of crystalline sodium trihydrogen selenite $NaH_3(SeO_3)_2$ (STHS) were reported for the first time by Pepinsky and Vedam [1] in 1959. The crystal, belonging, at room temperature, to the monoclinic system, exhibits a ferroelectric phase transition at 194 K. Ferroelectric activity was observed from this temperature down to that of liquid nitrogen. The nonpolar phase of the crystal, called the α-phase, was reported to be monoclinic, the point group being $2/m$ with two formula units per unit cell [1]. The system of crystallographic axes (a, b, c) proposed by Miki [2] is presented in figure 1.

The system of orthogonal crystallophysic axes (x, y, z) was proposed by Shuvalov *et al* [3, 4]. The x- and y-axes are directed along the acute and obtuse bisectrices of the optical axes angle at room temperature, whereas the z-axis is perpendicular to the optical axes plane. The y-axis coincides with the crystallographic b-axis for a monoclinic crystal. The same coordinate system has been accepted in this work.

On cooling, the STHS crystal undergoes two structural phase transitions. At the first one, mentioned above, the crystal becomes electrically multiaxial (β-phase). The spontaneous
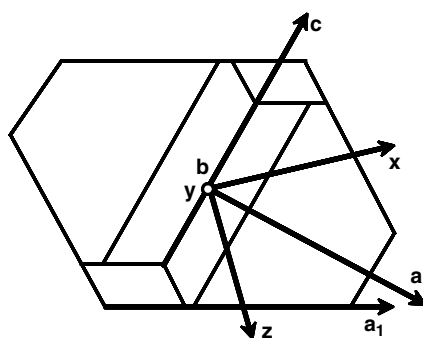
Figure 1. The STHS crystal habit and the relation between the coordinate axes x, y, z and the crystallographic axes $a, b,$ and c.

polarization appears in three directions (x, y and z) and the crystal symmetry changes to the triclinic point group 1 (the space group $P1$) [2, 3]. Whereas the x- and y-components of the spontaneous polarization are comparable ($P_{sx} = 3.1 \ \mu C \ cm^{-2}$, $P_{sy} = 3.8 \ \mu C \ cm^{-2}$ [4]) the z-component is relatively small ($P_{sz} = 0.2 \ \mu C \ cm^{-2}$). Consequently, the direction of the P_s-component in the xz-plane is almost parallel to the x-axis.

An NMR study [5] showed that the unit cell dimensions in the β-phase are doubled along both, the a- and b-axes, with respect to the dimensions in the α-phase. At a temperature of about 100 K the crystal undergoes a second phase transition to another phase (γ-phase) with a symmetry change from 1 to m [2–10]. In the γ-phase, the crystal is still a ferroelectric but the spontaneous polarization component P_{sy}, as well as the doubling of the unit cell in the a direction, disappears [5]. The dielectric constants ε_x and ε_y show a temperature hysteresis (of about 10 K) at the low-temperature phase transition, characteristic for transitions of the first-order type. It should be noted that no temperature hysteresis has been observed at the $\alpha \leftrightarrow \beta$ transition [3].

Blinc *et al* [11] and independently Gavrilova *et al* [12] reported that the replacement of hydrogen by deuterium shifts the Curie point of the crystal from 194 to 270.5 K. That significant isotopic effect proves that the hydrogen bonds play an essential role as triggers at the ferroelectric phase transition. From the NMR study it was concluded that the transition is accompanied by an ordering of hydrogens as well as by a distortion of the SeO_2^- and Na^+ network [5]. The selenite ions can be assumed to be linked together by hydrogen bonds on layers forming a two-dimensional structure connected closely with a plane to which the direction of spontaneous polarization is parallel. The specific heat measurements and the entropy calculations confirm the essential role of hydrogen bonds at the phase transition [13].

In the ferroelectric β-phase there are four possible directions of the P_s vector, and the crystal is electrically biaxial. Since the high-symmetry and low-symmetry structures belong to different crystal systems the phase transition is a ferroelastic one. Two systems of ferroelastic domain are observed in the β-phase: y-domains twinned along the former two-fold axis and m-domains twinned along the former mirror plane [3, 14]. A system of ferroelectric domains with antipolar directions of P_s inside the ferroelastic domains is created. The slopes of the P_s vectors with respect to the ferroelastic domain walls are different for the y- and m-domains, and the twinning of the two systems of antipolarized domains is more preferential along the xz-plane than along the y-axis [3]. The dielectric properties studies performed by different authors [3, 15–17] confirm a considerable domain contribution to the dielectric constant value. The ferroelastic domain structure evolution under an electric field of 50 Hz was observed [18].

The external electric field changes not only the orientation of P_s in the ferroelectric domain substructure, but also causes the reorganization of the ferroelastic domain system. Under an E_x field only y-domains, while under an E_y field only m-domains, are observed in the crystal. The rebuilding of the y-domain system into the m-domain system, or vice versa, was observed for the electric field range of 0.2–0.3 kV cm^{-1}. As a result, the electrically charged domain walls disappear in the crystal.

Despite STHS being a rare example of a crystal which is electrically uniaxial in one ferroelectric phase (γ) and electrically multiaxial in the other one (β), not all its physical properties have been researched and explained. Two research fields appear worthy of interest. The first one is the dielectric response of the crystal in the β phase strongly influenced by the domain texture. The second is the crystal properties in the vicinity of the ferroelectric phase transition. The lack of the transition thermal hysteresis and the rapid, but continuous, increase of P_s at the phase transition led the same authors [3, 17] to the conclusion that the transition is of the second order but is close to one of the first order. However, in other studies of the crystal, the transition was classified as a first-order transition [16, 19].

In the paper the results of measurements of spontaneous polarization and electric permittivity, as well as the observations of domain texture of STHS crystal, are presented.

2. Experimental details

From a stoichiometric amount of SeO_2 and NaOH dissolved in water after evaporation, polycrystals of $NaH_3(SeO_3)_2$ were obtained. From the polycrystals a saturated water solution was prepared and then a single crystal was grown by evaporation at a stable temperature, 303 K. Plates of about 1 mm thickness were cut out from the crystal in such a way that the main surface of the plate was perpendicular to the x-, y- and P_s direction (x-, y-, and P_s samples, respectively). For the dielectric measurements the main surfaces of the samples were covered with a silver conducting paste. The sample was hung in the nitrogen gas chamber of a cryostat with the help of two thin cooper wires which were also used as the electrical contacts. The temperature in the chamber was controlled with an accuracy not worse than 0.01 K. The temperature was measured using a copper–constantan thermocouple connected to an HP 34420A nanovolt/microhm meter. The hot point (end) of thermocouple was placed in the cryostat chamber, close to the sample, or was glued to the sample surface.

The domain texture was observed in the uniaxial optical cryostat using a polarizing microscope. The cryostat made the dielectric measurements possible during the optical observations.

The sample electric capacity was measured using a precision LCR-meter HP 4284A, with a measuring field of 10 V cm^{-1} in amplitude and 1 kHz in frequency, allowing us to calculate the dielectric constant value ε. The temperature dependence of ε was measured during a cooling run with a rate of 0.5 K min^{-1} under a bias electric field up to 1100 kV m^{-1}.

The hysteresis loops were registered at 0.01 Hz using an electrometer and at 50 Hz using a classical Sawyer–Tower circuit. The temperature dependence of the spontaneous polarization was also obtained from pyroelectric current measurements.

3. Results and discussion

3.1. Evidence of the first-order character of the ferroelectric phase transition

The sample temperature measured during the cooling and heating run with the constant rates is presented in figure 2.
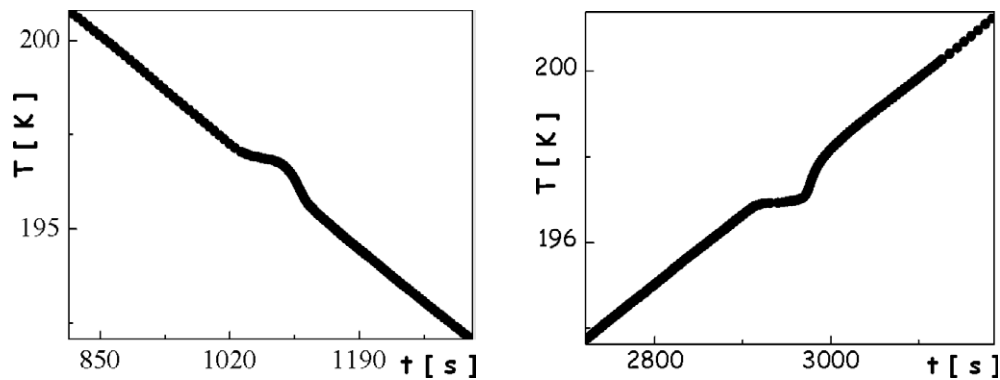
Figure 2. The sample temperature variations during cooling and heating with constant rates.
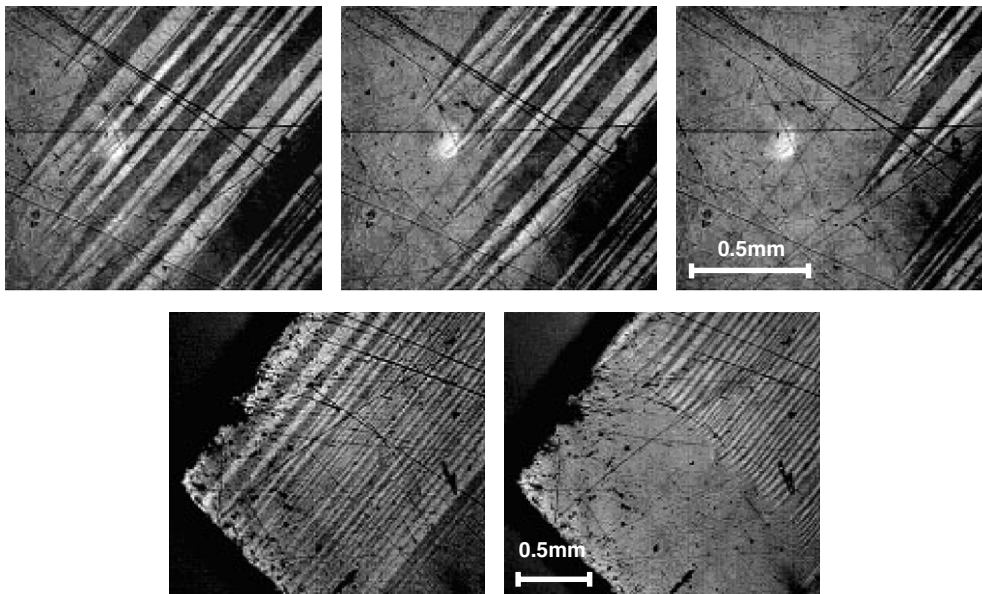

Figure 3. The *m*-domain system observed during the phase transition from the ferroelectric to the paraelectric phase.

When the gas temperature in the cryostat chamber was changed linearly with time, the sample temperature showed a deviation from linear dependence in the phase transition region. Such a phenomenon is characteristic for a first-order phase transition and it clearly appears that the crystal temperature stays approximately constant during the phase coexistence. It is necessary to change the surrounding gas temperature to bring the thermal energy variation necessary for the phase transition [20].

Observation of the domain structure in the *z* direction provides evidence of phase coexistence during the ferroelectric phase transition. In figure 3 the *m*-domain system observed during the phase transition is presented. The phase coexistence, characteristic for a first-order phase transition, is clearly visible. Unfortunately, the observation in the *z*-direction does not directly reveal the phase front position and its shape.
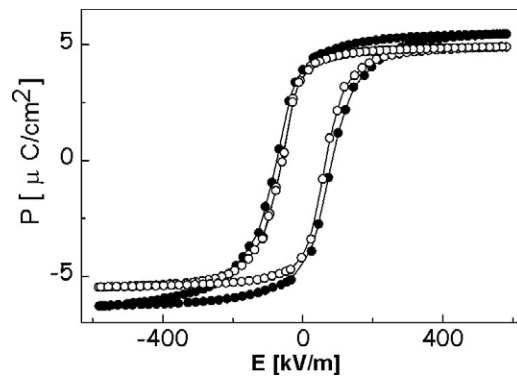
Figure 4. The hysteresis loops obtained for the P_s-sample at 0.01 Hz (black points: 167.9 K; white points: 195.7 K).
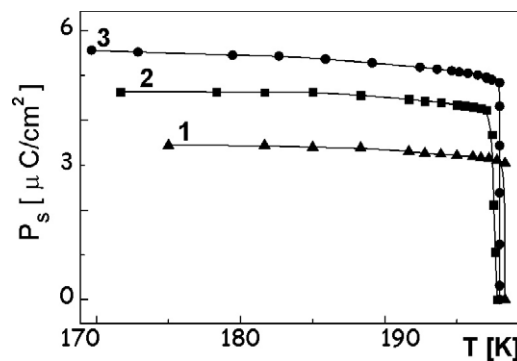

Figure 5. Low-frequency measurement of spontaneous polarization components. 1: P_{sx}; 2: P_{sy}; 3: P_s.

3.2. The spontaneous polarization measurements

Two examples of hysteresis loop registered for the P_s-sample at 0.01 Hz are presented in figure 4. The loops obtained for the x- and y-samples were similar in shape. The spontaneous polarization values obtained in this way are presented in figure 5.

The obtained values of spontaneous polarization components at 180 K, $P_{sx} = 3.4$ μC cm^{-2} and $P_{sy} = 4.6$ μC cm^{-2} are higher with respect to those in [3]. The presented results have been obtained for the samples cut out from a rather young STHS crystal. In further experiments the spontaneous polarization components values were lower and comparable with those obtained by Shuvalov *et al* [3]. This can indicate a considerable ageing process in the crystal. The ratio P_{sx}/P_{sy} is practically independent of temperature and allows us to find the direction of P_s in the xy-plane.

The lack of temperature hysteresis during the $\alpha \leftrightarrow \beta$ phase transition observed by Shuvalov *et al* [3] cannot be confirmed. A hysteresis of about 1 K has been found in the temperature dependence of the electric permittivity [16]. During the pyroelectric measurements the hysteresis was even larger. The results presented in figure 6, showing a hysteresis of 2.64 K, were obtained for cooling and heating rates of 0.2 K min^{-1}. The thermal hysteresis magnitude depends on the cooling and heating rate and the largest observed in our experiment was of about 7 K.
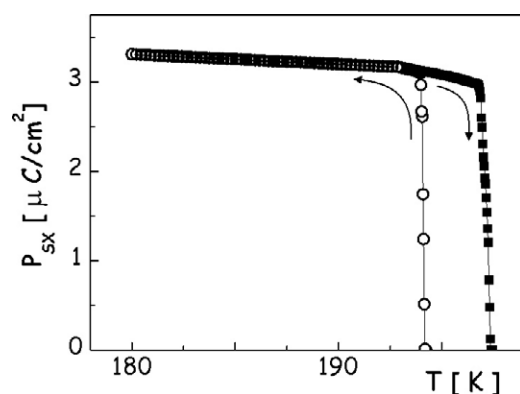
Figure 6. The temperature dependence of P_{sx} obtained by pyroelectric measurements.
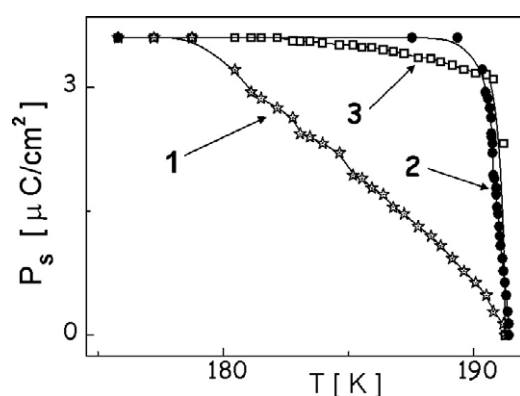

Figure 7. Temperature variations of spontaneous polarization obtained for the P_s-sample (see description in the text).

During the measurements of the hysteresis loops at 50 Hz electric field an important heating effect was revealed. It was observed for all samples but the biggest one was for the P_s-sample. The results obtained for the sample are presented in figure 7.

The spontaneous polarization obtained for 50 Hz electric field, as a function of the cryostat chamber temperature, is presented by curve 1. For comparison the spontaneous polarization obtained from 0.01 Hz hysteresis loops as a function of the cryostat chamber temperature is shown (curve 3). The pronounced discrepancy between curves 1 and 3 indicates the considerable heating effect under the electric field of 50 Hz. To prove this, the sample temperature changes were measured while reversing the crystal polarization by an alternating electric field of 500 kV m^{-1}. The sample temperature increases and stabilizes after about 1 min. The temperature increase ΔT is almost constant far from the phase transition and it decreases on approaching the phase transition temperature. The results obtained for the P_s-sample are presented in figure 8. The effect was smaller for x- and y-samples and the noted maximum increase of temperature was 4.5 and 2.5 K respectively. In figure 7 curve 2 illustrates the same results as curve 1 but presented versus the temperature of the sample $(T + \Delta T)$. The presented results show that we are dealing with a temperature stabilization effect. The alternating electric field of amplitude higher than a coercive field stabilizes the sample temperature close to the phase transition temperature.
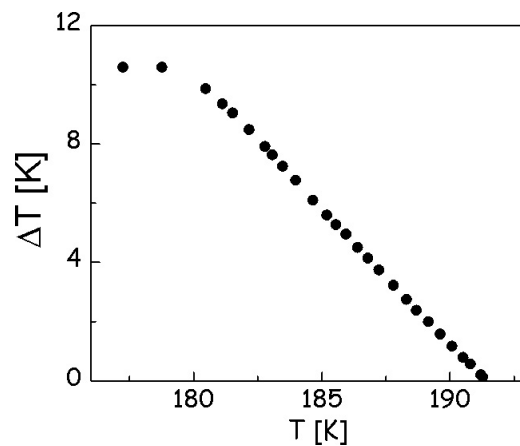
Figure 8. The increase of the P_s-sample temperature during polarization reversal under 50 Hz electric field.

Contrary to appearance, the results presented in figure 7 (curves 1 and 2) cannot be interpreted as proving the continuous changes of P_s close to the phase transition temperature. The polarization values presented in the figure were obtained from the hysteresis loops in the same classical way as the spontaneous polarization values are estimated (the saturation value of the electric displacement extrapolated to zero field). However, from the simultaneous observation of the ferroelastic domain structure it has been concluded that the rapid, but continuous, increase of the hysteresis loop height is observed in the phase coexistence region. This means that only a certain part of the sample volume is polarized and the values of polarization obtained from hysteresis loops cannot be considered as the spontaneous polarization values.

Assuming that we can conclude that the polarization reversal leads to considerable heating of the crystal, much greater than observed for other ferroelectric crystals. As a result the sample temperature increases and stabilizes in the phase coexistence region when the heating rate decreases and becomes the same as the heat exchange between sample and the thermal bath. The sample heating is probably connected with the mechanical constraints and deformations caused by the alternating electric field. As was mentioned, the external electric field leads to rebuilding not only the ferroelectric domains structure but also the ferroelastic one. This results in important stresses which sometimes, in the low-temperature region, destroy the sample.

3.3. The electric permittivity measurements

The temperature variations of dielectric constants obtained for the x-, y- and P_s-samples are presented in figures 9 and 10. In the paraelectric phase near the phase transition, the Curie–Weiss law is fulfilled with constants

$$C_x = (6.1 \pm 0.3) \times 10^3 \text{ K}$$
$$C_y = (9.8 \pm 0.3) \times 10^3 \text{ K}$$
$$C_{Ps} = (13.8 \pm 0.5) \times 10^3 \text{ K}$$

respectively for the x-, y- and P_s- samples. Such values of the Curie–Weiss constant, which mirror the weak dielectric constant dependence on temperature, are characteristic rather for order–disorder phase transitions than for displacive-type transitions [21].
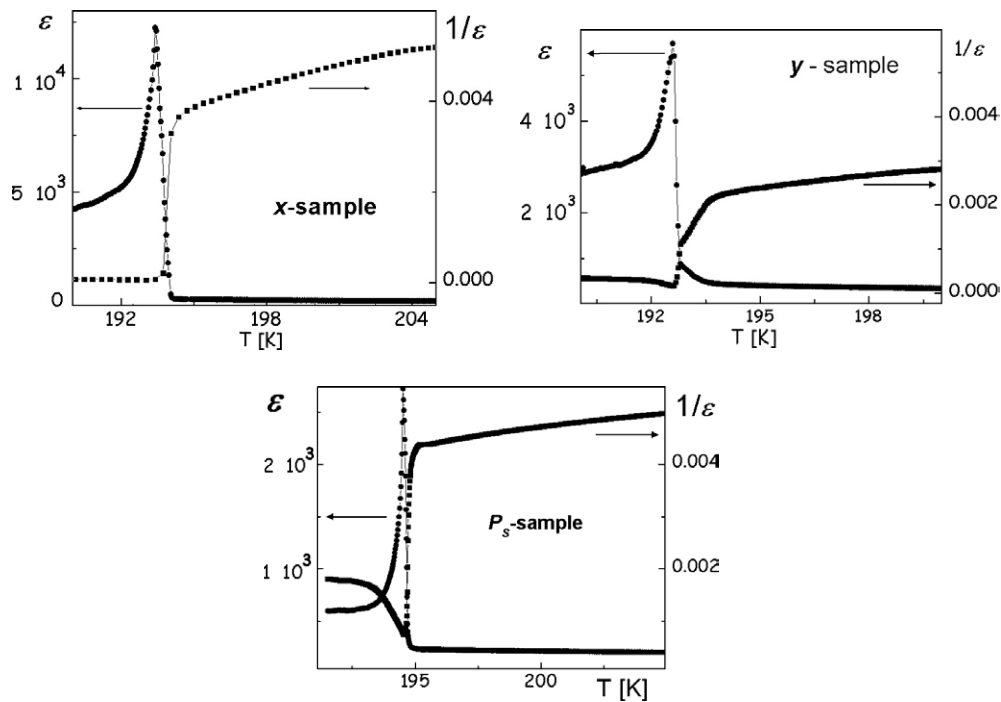
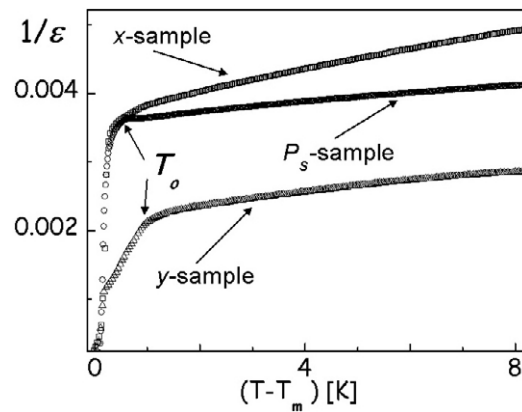**Figure 9.** Temperature variation of the dielectric constant and its reciprocal obtained while cooling.

Figure 10. Temperature variation of the reciprocal dielectric constant in the paraelectric phase (T_m:-temperature corresponds to the maximum of ε).

A drastic increase of ε along all directions accompanies the phase transition. Such a behaviour was earlier observed for a DKDP (KD_2PO_4) crystal and it was explained by the effect of the domain structure and the phase front on the dielectric response of the crystal [20, 22]. When the phase front appears in the sample the dielectric constant increases rapidly, reaching a maximum value when the domain structure is created in the whole volume of the sample [20]. We can suppose, by analogy, that the phase transition in the STHS crystal starts at temperature T_0 marked in figures 10 and 11.
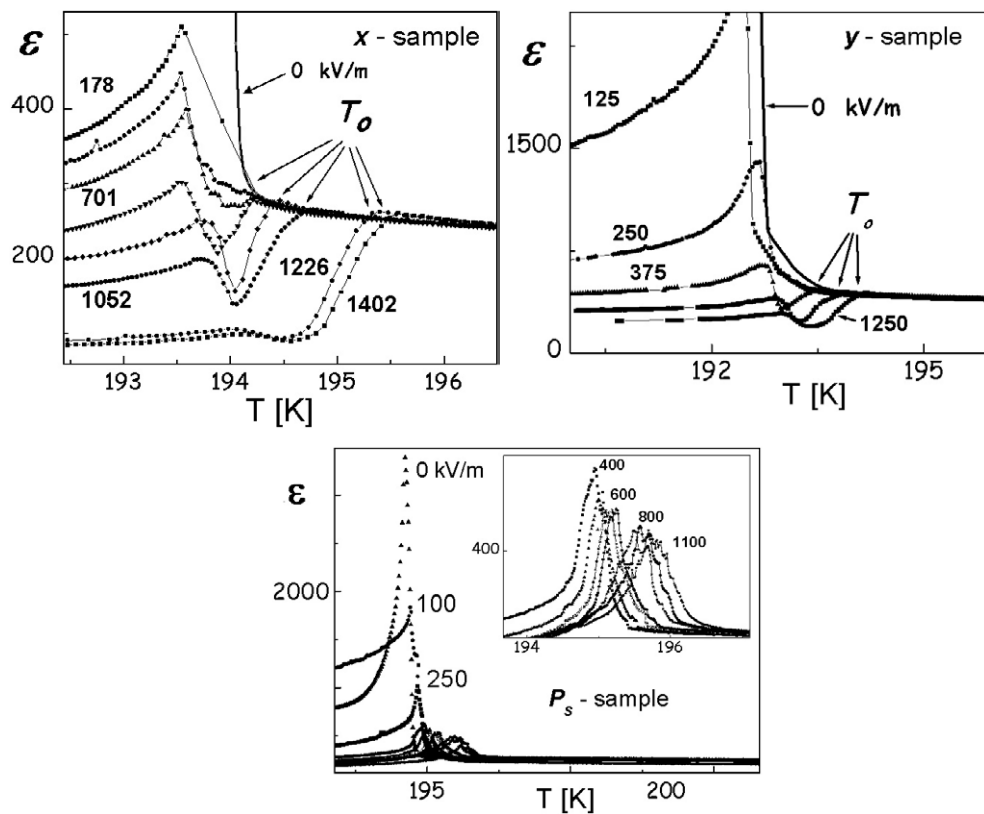
Figure 11. Temperature variations of the dielectric constant at various dc electric fields (values in kV m^{-1}).

To show the domain texture effect on the dielectric constant clearly, measurements under dc electric fields E were performed. The temperature dependence of ε, measured in the x- and y-directions, changes its character when the electric field value increases. The results are presented in figure 11, where the voltage is a parameter for the individual curves (the samples thickness were 0.57 and 0.80 mm for the x- and y-sample, respectively). The solid lines present the results obtained at zero dc field. Initially, the electric field decreases the maximum of ε and shifts it towards high temperatures. For higher electric fields the phase transition starts at the temperature T_0 with a decreasing of ε, which after passing a minimum reaches its maximum value at T_m. It can be supposed that in the temperature range (T_0, T_m) phase coexistence takes place and at temperature T_m the whole volume of the sample is occupied by the ferroelectric phase. In figure 11 the dielectric constant is presented as a function of the thermal bath temperature. Taking into consideration the results presented in figure 2, it clearly appears that the phase coexistence region is really very narrow and the phase transition, in first approximation, can be considered as an isothermal process.

Whereas the electric field effects on the x- and y-samples are similar, the behaviour of the P_s-sample under dc electric field is quite different. The maximum of ε decreases and shifts towards higher temperatures, but a characteristic minimum of ε is not observed. It should be noted that the electric field applied in the P_s-direction is effectively applied mutually in the x- and y-directions. In such a situation none of the ferroelastic domain system is privileged.
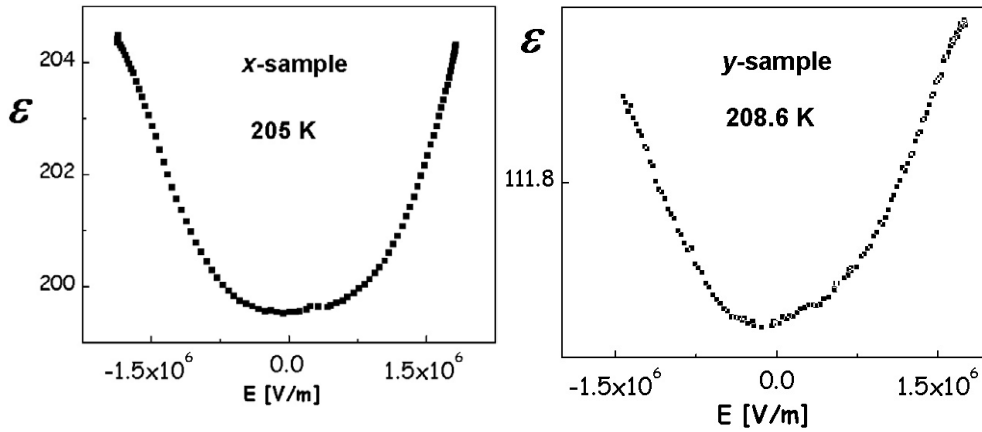
Figure 12. Effect of dc bias field on the dielectric constant of STHS crystal (chosen examples).

To analyse the nonlinear dielectric properties of the crystal the dielectric constant was measured as a function of electric field at several temperatures in the paraelectric phase. The examples of results obtained for x- samples (205 K) and y-samples (208.6 K) are presented in figure 12.

The increase of ε with electric field starting from zero value is characteristic for ferroelectric crystals undergoing a first-order phase transition. The dielectric constant reaches its maximum value at a certain electric field, characteristic for the crystal, and then decreases while the electric field increases. In our experiment the electric field range was not sufficiently large to attain the maxima of ε. A detailed discussion of that dielectric behaviour of ferroelectric crystals was presented by Tchukvinskyi *et al* [23].

As the expression for the free energy for such a multiaxial ferroelectric–ferroelastic crystal is very complex [24], a quantitative analysis of the dielectric properties can be done starting from the 'partial' dielectric state equations, corresponding to different electric field orientations with respect to the crystal.

$$E_i = A_i(T - T_c)D_i + B_i D_i^3 \tag{1}$$

where $i = x, y$ refers to the different experimental situations described above, E_i and D_i are the electric field and electric displacement in chosen directions, and A_i and B_i are coefficients characteristic for the crystal and the sample orientation which can be determined experimentally. From equation (1) we deduce the reciprocal permittivity

$$\varepsilon_i^{-1} = A_i(T - T_c) + 3B_i \cdot D_i^2. \tag{2}$$

In these both equations D_i includes the field-induced as well as the spontaneous polarization. Having eliminated the electric displacement and the temperature we obtain the dielectric state equation for the paraelectric phase in the scaling form

$$f(\varepsilon_i) = \left(\frac{1}{\varepsilon_i(E_i)}\right)^3 + 3\frac{1}{\varepsilon_i(0)}\left(\frac{1}{\varepsilon_i(E_i)}\right)^2 - 4\left(\frac{1}{\varepsilon_i(0)}\right)^3 = 27B_iE_i^2 \tag{3}$$

which allows us to determine the value of the nonlinearity coefficient B_i [25]. This approach, correct for a ferroelectric crystal undergoing a second-order phase transition, in the case of our crystal has only descriptive character limited by temperature and the electric field range. However, the confrontation of the experimental data with that formalism can be interesting and it allows a quantitative description of the dielectric properties of the crystal, particularly the
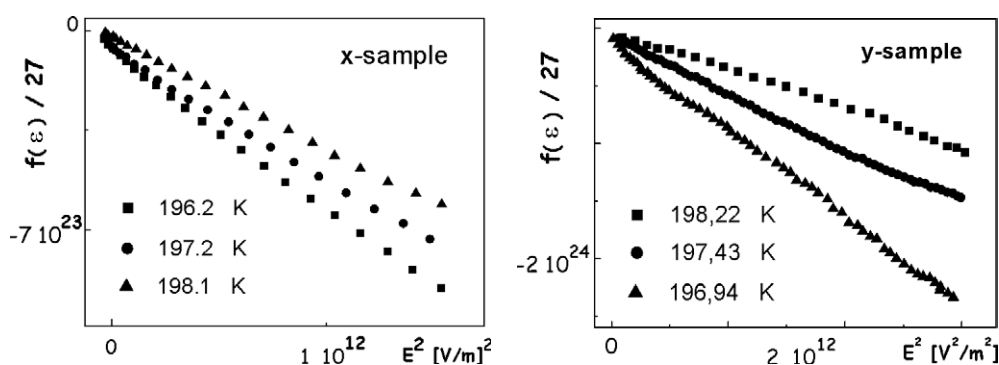
Figure 13. Examples of the field dependence of electric permittivity in the paraelectric phase presented according to equation (3).
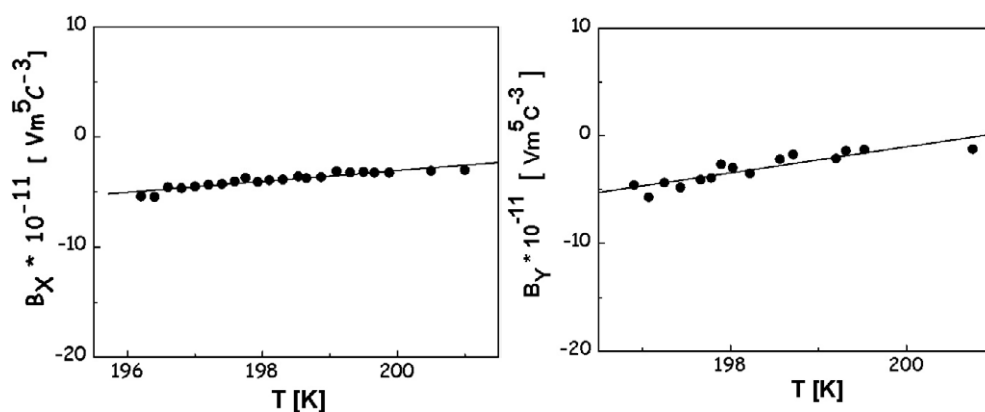

Figure 14. The nonlinearity coefficients B_x and B_y obtained from the isothermal field dependences of the electric permittivity.

isothermal field dependences of the electric permittivity. The following values of coefficients A_i can be obtained from the Curie–Weiss constants presented above:

$$A_x = (1.8 \pm 0.2) \times 10^7 \ (\text{V m C}^{-1} \text{ K}^{-1})$$
$$A_y = (1.1 \pm 0.1) \times 10^7 \ (\text{V m C}^{-1} \text{ K}^{-1}).$$

The results presented in figure 13 prove that in the electric field range applied in the experiment equations (1)–(3) can be used for the phenomenological description of the STHS crystal. The nonlinear coefficients B_i for all types of samples are negative, as could be expected. Obtained values of B_i are presented in figure 14. For both orientations of the crystal with respect to electric field, B_i varies linearly with temperature above the phase transition temperature, similarly to what was found earlier for BaTiO$_3$ [26] and DMAGaS ((CH$_3$)$_2$NH$_2$Ga(SO$_4$)$_2$·6H$_2$O) [23] crystals.

From the linear approximation of $B_i(T)$ to the phase transition temperature the following values were obtained:

$$B_x(T_0) = -5.0 \times 10^{11} \ (\text{V m}^5 \text{ C}^{-3})$$
$$B_y(T_0) = -5.8 \times 10^{11} \ (\text{V m}^5 \text{ C}^{-3}).$$

Table 1. All obtained parameters.

	A_0 (V m C^{-1} K^{-1})	B (V m^5 C^{-3})	C (V m^9 C^{-5})	$P_s(T_0)$ (10^{-2} C m^{-2})	ΔT (K)
x-sample	$(1.8 \pm 0.2) \times 10^7$	-5.0×10^{11}	4.1×10^{14}	3.04	8.5
y-sample	$(1.1 \pm 0.1) \times 10^7$	-5.8×10^{11}	2.7×10^{14}	4.23	27.1

In the next step, the coefficients C_i can be estimated from the value of spontaneous polarization at the phase transition temperature as $P_s^2(T_0) = 3B/4C$ [27]. The obtained values are

$$C_x = 4.1 \times 10^{14} \text{ (V m}^9 \text{ C}^{-5})$$
$$C_y = 2.7 \times 10^{14} \text{ (V m}^9 \text{ C}^{-5}).$$

All obtained parameters are collected in the table 1.

The two kinds of sample differ most strikingly in the magnitude of the maximum possible thermal hysteresis $\Delta T = B^2/4A_0C$. As the experimentally observed thermal hysteresis does not exceed 8.5 K, it can be concluded that the x-component of spontaneous polarization plays a predominant role at the ferroelectric phase transition.

4. Summary

Our studies of crystalline sodium trihydrogen selenite indicate clearly that upper phase transition is of first order. That conclusion can be drawn from the following experimental results:

- the sample temperature variations during cooling and heating with constant rates (temperature stabilization during the phase transition),
- the phase coexistence at the phase transition temperature,
- the hysteresis observed in the temperature dependence of electric permittivity and during the pyroelectric measurements,
- the behaviour of ε under dc electric field,
- the negative value of the nonlinear coefficients B_i for all types of sample.

During the measurements of the hysteresis loops in 50 Hz electric field an important heating effect, much greater than observed for other ferroelectric crystals, has been revealed. The sample heating is probably connected with the mechanical constraints and deformations caused by the alternating electric field.

The temperature dependence of ε, measured in the x- and y-directions, has been measured. The electric field decreases the maximum of ε and shifts it towards high temperatures. For higher electric fields the phase transition starts at the temperature T_0 with a decreasing of ε, which after passing a minimum reaches its maximum value at T_m. The behaviour of the P_s-sample under dc electric field is quite different. The maximum of ε decreases and shifts towards higher temperatures, but a characteristic minimum of ε is not observed.

References

[1] Pepinsky R and Vedam K 1959 *Phys. Rev.* **114** 1217
[2] Miki H 1973 *J. Phys. Soc. Japan* **34** 1314
[3] Shuvalov L A and Ivanov N R 1967 *Phys. Status Solidi* **22** 279
[4] Shuvalov L A, Ivanov N R, Kirpichnikova L F and Schagina N M 1972 *Kristallografiya* **17** 966
[5] Blinc R, Stepišnik J and Zupančič I 1968 *Phys. Rev.* **176** 732

[6] Makita Y 1964 *J. Phys. Soc. Japan* **19** 576
[7] Makita Y, Vedam K and Pepinsky R 1962 *Bull. Am. Phys. Soc.* **II7** 241
[8] Ivanov N R, Shuvalov L A, Fedosyuk R M and Pluzhnikov K A 1963 *Proc. R. Soc.* A **276** 258
[9] Ivanov N R, Shuvalov L A, Fedosyuk R M and Pluzhnikov K A 1966 *Zh. Eksp. Teor. Fiz. Pis. Red.* **4** 220
[10] Blinc R, Levstik A, Stepišnik J, Trontelj Z and Zupančič I 1968 *Phys. Lett.* A **26** 290
[11] Blinc R and Vovk D 1965 *Phys. Lett.* **19** 177
[12] Gavrilova-Podolskaya G V, Yudin A L and Lundin A G 1965 *Zh. Eksp. Teor. Fiz. Pis. Red.* **1** 36
[13] Makita Y and Miki H 1970 *J. Phys. Soc. Japan* **28** 1221
[14] Kirikov W A, Shuvalov L A, Zheludev I S, Gvozdober R S and Petrov W I 1975 *Izv. Akad. Nauk SSSR Ser. Fiz.* **39** 1015
[15] Shuvalov L A, Ivanov N R, Kirpichnikova L F and Schagina M N 1972 *Kristallografiya* **17** 966
[16] Pykacz H, Czapla Z and Mróz J 1978 *Acta Phys. Pol.* A **53** 387
[17] Blinc R, Javonovic A, Levstik A and Prelesnik A 1965 *J. Phys. Chem. Solids* **26** 1359
[18] Askonchesky A A, Kirikov W A and Shuvalov L A 1971 *Izv. Akad. Nauk SSSR Ser. Fiz.* **35** 1877
[19] Malecka A, Stankowska J and Shuvalov L A 1976 *Bull. Acad. Pol. Sci. Sér. Sci. Math. Astron. Phys.* **24** 143
[20] Bornarel J and Cach R 1999 *Phys. Rev.* B **60** 3806
[21] Nakamura E, Mitsui T and Furuichi J 1963 *J. Phys. Soc. Japan* **18** 1477
[22] Bornarel J and Cach R 2003 *J. Phys.: Condens. Matter* **15** 4371
[23] Tchukvinskyi R, Cach R and Czapla Z 1998 *Z. Naturf.* A **53** 105
[24] Sasaki Y 1991 *J. Phys. Soc. Japan* **60** 539
[25] Cach R, Jaśkiewicz A and Lamber R 1982 *Acta Phys. Pol.* A **62** 249
[26] Drougard M E, Landauer R and Young D R 1955 *Phys. Rev.* **98** 1010
[27] Lines M E and Glass A M 1977 *Principles and Applications of Ferroelectrics and Related Materials* (Oxford: Clarendon)